



Penetration of dipole radiation into an ENZ medium

Henk F. Arnoldus

Department of Physics and Astronomy, Mississippi State University, P.O. Box 5167, Mississippi State, MS, 39762-5167, USA

ARTICLE INFO

Keywords:

Epsilon-near-zero medium
Dipole radiation
Poynting vector
Fresnel coefficients

ABSTRACT

We consider electric dipole radiation emitted near an interface with an epsilon-near-zero (ENZ) material. Such a medium is nearly impenetrable for electromagnetic plane waves, but we show that dipole radiation can penetrate deep into the medium. The radiation is represented by an angular spectrum of plane waves, and each partial wave transmits as an evanescent wave. The sum of these waves, however, is not evanescent, but decays algebraically with the distance to the interface. We have evaluated the electric and magnetic fields inside the material, and we have constructed the Poynting vector. We found that energy flows through the material, and not only in a small region near the interface. For the case of a perpendicular dipole, the magnetic field is zero, and the electric field can be obtained in closed form. We show that the electric field decays as the third power of the distance to the interface.

1. Introduction

An epsilon-near-zero (ENZ) material has a near-zero index of refraction. When an electromagnetic plane wave with angular frequency ω is incident upon an interface with an ENZ medium, all radiation is reflected. The Fresnel reflection coefficients R_s and R_p for s and p waves, respectively, are equal to unity in magnitude. Upon reflection, a phase shift occurs, but no radiative energy penetrates the material. Inside the material, there can still be electric and magnetic fields, but these are confined to a small layer near the interface. These evanescent fields decay exponentially into the material, and they propagate into the direction parallel to the interface. An exception to this general picture occurs for a plane wave at near normal incidence [1]. An electric field is present throughout the ENZ material, but the magnetic field is identically zero. The electric field oscillates with angular frequency ω , but it has no spatial dependence. This peculiar phenomenon is referred to as ‘static optics’. For a material with near-zero refractive index, the wave number in the material is near-zero, and therefore the wavelength approaches infinity. Consequently, the electric field in the material can have no spatial dependence. Since the magnetic field is zero, the Poynting vector is zero, and no energy flow is associated with this oscillating electric field.

ENZ materials have been predicted to have a host of interesting properties. With the quasi-static field that is transmitted into the material at near normal incidence, it should be possible to tunnel radiation through the material without loss of phase information [2–7]. This would allow for transmission through bends of arbitrary shape. Since this radiation only transmits at near normal incidence, it should be possible to construct angular filters based on this principle [8–11]. Most notably, an electric dipole may levitate when it is located close

to the interface of an ENZ material [12–15]. Metamaterial ENZ media have been constructed in the microwave and terahertz regions of the spectrum [16–20], and more recently in the optical region [21–23].

The notion that ENZ materials are impenetrable for radiation derives from the consideration of traveling incident plane waves. We shall consider electric dipole radiation, which contains both traveling and evanescent waves. The evanescent reflected dipole waves are responsible for the predicted levitation. Here we shall investigate the possible transmission of electric dipole radiation into an ENZ medium. In an angular spectrum representation, the dipole field is a superposition of traveling and evanescent plane waves. These waves are incident upon the ENZ interface, and each wave transmits into the medium as an evanescent wave. It may therefore stand to reason that the transmitted dipole field is evanescent, and no energy can propagate into the material. We shall show that this is not the case.

2. Dipole near an interface

An oscillating electric dipole has a dipole moment

$$\mathbf{d}(t) = \text{Re}(\mathbf{d}e^{-i\omega t}), \quad (1)$$

with \mathbf{d} the complex amplitude. We consider the dipole to be located a distance H from an interface, as shown in Fig. 1. The dipole is embedded in a medium with (relative) permittivity ϵ_1 , assumed to be positive, and the medium has a permittivity ϵ_2 . The interface is the xy plane, and the positive z axis is taken as shown in the figure. The incident dipole radiation, symbolically represented by the wave vector \mathbf{k}_i , is a superposition of traveling and evanescent waves. The evanescent waves decay in the positive z direction, as schematically

E-mail address: hfa1@msstate.edu.

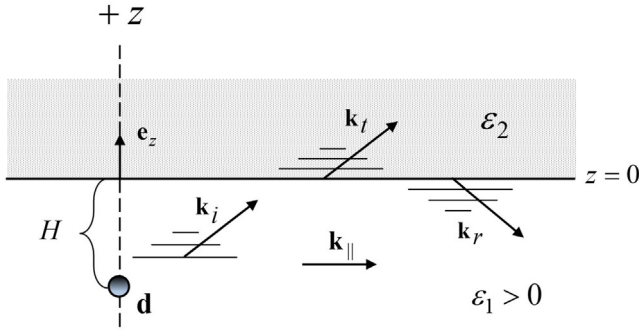


Fig. 1. Shown is the setup of a dipole near the interface with a medium. Each partial incident dipole wave reflects at the interface and transmits through the interface.

indicated by the horizontal lines. Each partial dipole wave reflects (\mathbf{k}_r) at the interface, and part of the incident radiation is transmitted into the medium (\mathbf{k}_t). Due to boundary conditions, each of the three wave vectors must have the same parallel component k_{\parallel} . The relative amplitudes of the reflected and transmitted waves, with respect to the incident wave, are expressed as Fresnel reflection coefficients R_{σ} and transmission coefficients T_{σ} , where $\sigma = s$ or p indicates the polarization of the wave.

We shall consider a dipole moment \mathbf{d} which lies in the yz plane, and we set $\mathbf{d} = d_0 \hat{\mathbf{u}}$ with $d_0 > 0$ and $\hat{\mathbf{u}} \cdot \hat{\mathbf{u}} = 1$. When $\hat{\mathbf{u}}$ is real, this represents a linear dipole, and when $\hat{\mathbf{u}}$ is complex, this is an elliptical dipole. In the region below the interface, the electric and magnetic fields are superpositions of the source fields and the reflected fields, and in the medium the fields are the transmitted fields by the interface. We shall set

$$\mathbf{E}(\mathbf{r}) = \zeta \tilde{\mathbf{E}}(\mathbf{r}), \quad (2)$$

$$\mathbf{B}(\mathbf{r}) = \frac{\zeta}{c} \tilde{\mathbf{B}}(\mathbf{r}), \quad (3)$$

for the complex amplitudes of the electric and magnetic fields, and here the overall constant ζ is defined as

$$\zeta = \frac{k_0^3 d_0}{4\pi \epsilon_0}, \quad (4)$$

with $k_0 = \omega/c$ as the wave number in free space. We shall consider the fields in the yz plane.

The source field is the field of a dipole embedded in a medium with permittivity ϵ_1 , and is given by

$$\tilde{\mathbf{E}}_s = \left\{ \hat{\mathbf{u}} - (\hat{\mathbf{q}}_1 \cdot \hat{\mathbf{u}}) \hat{\mathbf{q}}_1 + [\hat{\mathbf{u}} - 3(\hat{\mathbf{q}}_1 \cdot \hat{\mathbf{u}}) \hat{\mathbf{q}}_1] \frac{i}{n_1 q_1} \left(1 + \frac{i}{n_1 q_1} \right) \right\} \frac{e^{i n_1 q_1}}{n_1 q_1}, \quad (5)$$

$$\tilde{\mathbf{B}}_s = (\hat{\mathbf{q}}_1 \times \hat{\mathbf{u}}) \left(1 + \frac{i}{n_1 q_1} \right) \frac{e^{i n_1 q_1}}{n_1 q_1}. \quad (6)$$

Here, $\mathbf{q}_1 = \bar{y} \mathbf{e}_y + (\bar{z} + h) \mathbf{e}_z$, with $\bar{y} = k_0 y$, $\bar{z} = k_0 z$, is the dimensionless position vector of the field point with respect to the location of the dipole, and $q_1 = |\mathbf{q}_1|$, $\hat{\mathbf{q}}_1 = \mathbf{q}_1/q_1$. The parameter $h = k_0 H$ is the dimensionless distance between the dipole and the interface, and $n_1 = \sqrt{\epsilon_1}$ is the index of refraction of the embedding medium.

The reflected and transmitted fields can be found by expanding the source fields of Eqs. (5) and (6) in an angular spectrum representation. Each partial wave is a polarized plane wave which is incident upon the interface, and the reflected and transmitted fields can be constructed with the help of Fresnel reflection and transmission coefficients for plane waves. In an angular spectrum representation, the wave vector \mathbf{k}_{\parallel} from Fig. 1 is the integration (superposition) variable, and $\alpha = k_{\parallel}/k_0$ is its dimensionless magnitude. The Fresnel coefficients depend on α , and are explicitly

$$R_s(\alpha) = \frac{v_1 - v_2}{v_1 + v_2}, \quad (7)$$

$$R_p(\alpha) = \frac{\epsilon_2 v_1 - \epsilon_1 v_2}{\epsilon_2 v_1 + \epsilon_1 v_2}, \quad (8)$$

$$T_s(\alpha) = \frac{2v_1}{v_1 + v_2}, \quad (9)$$

$$T_p(\alpha) = n_2 \frac{2n_1 v_1}{\epsilon_2 v_1 + \epsilon_1 v_2}. \quad (10)$$

Here we have set

$$v_k = \sqrt{\epsilon_k - \alpha^2}, \quad k = 1, 2, \quad (11)$$

and $n_2 = \sqrt{\epsilon_2}$. The dimensionless z components of the wave vectors \mathbf{k}_i and \mathbf{k}_r , shown in Fig. 1, are v_1 and $-v_1$, respectively. Since we assume $\epsilon_1 > 0$, the value of v_1 is either positive or positive imaginary. For $0 \leq \alpha < n_1$, v_1 is real, and the incident and reflected waves are traveling. For $\alpha > n_1$, both waves are evanescent, and decay into the direction away from the interface. For a traveling incident wave we have $\alpha = n_1 \sin \theta_i$, with θ_i the angle of incidence, and for an evanescent incident wave, $1/\alpha$ is the (dimensionless) decay length of the exponentially decaying wave.

The reflected fields in the yz plane are found to be [24]

$$\tilde{\mathbf{E}}_r = u_y \mathbf{e}_y (\mathcal{R}_s^{(1)} + \mathcal{R}_p^{(1)}) + u_z \mathbf{e}_z \mathcal{R}_p^{(3)} + \text{sgn}(\bar{y}) (u_z \mathbf{e}_y - u_y \mathbf{e}_z) \mathcal{R}_p^{(4)}, \quad (12)$$

$$\tilde{\mathbf{B}}_r = -u_y \mathbf{e}_x (\mathcal{R}_s^{(4)} + \mathcal{R}_p^{(6)}) - \text{sgn}(\bar{y}) u_z \mathbf{e}_x \mathcal{R}_p^{(7)}. \quad (13)$$

The auxiliary functions $\mathcal{R}_{\sigma}^{(i)}$ are Sommerfeld-type integrals, and are defined in Appendix. They are functions of the dimensionless coordinates $\bar{\rho} = k_0 \rho$ and $\bar{z} = k_0 z$. The transmitted fields are

$$\tilde{\mathbf{E}}_t = u_y \mathbf{e}_y (\mathcal{T}_s^{(1)} + \mathcal{T}_p^{(1)}) + u_z \mathbf{e}_z \mathcal{T}_p^{(3)} + \text{sgn}(\bar{y}) u_z \mathbf{e}_y \mathcal{T}_p^{(4)} + \text{sgn}(\bar{y}) u_y \mathbf{e}_z \mathcal{T}_p^{(5)}, \quad (14)$$

$$\tilde{\mathbf{B}}_t = -u_y \mathbf{e}_x (\mathcal{T}_s^{(4)} + \mathcal{T}_p^{(7)}) - \text{sgn}(\bar{y}) u_z \mathbf{e}_x \mathcal{T}_p^{(8)}, \quad (15)$$

with the functions $\mathcal{T}_{\sigma}^{(i)}$ given in the Appendix. The electric fields are in the yz plane, and the magnetic fields are along the x axis.

3. Fresnel coefficients for an ENZ interface

For an ENZ medium we have $\epsilon_2 \rightarrow 0$, $n_2 \rightarrow 0$, and we now consider this limit. The first observation is that with Eq. (11) we have

$$v_2 = i\alpha. \quad (16)$$

Depending on α , the incident wave is traveling or evanescent. Since v_2 is the z component of the wave vector in the ENZ material, we conclude that all transmitted waves are evanescent. An exception is $\alpha = 0$, corresponding to normal incidence. Then $v_3 = 0$, so there is no z dependence in the transmitted wave. The wave travels along the xy plane, is constant in amplitude in the z direction, and oscillates with angular frequency ω . This is the *static optics* case of transmission into an ENZ medium.

With $v_2 = i\alpha$ we find from Eqs. (7) and (9) for s waves

$$R_s(\alpha) = \frac{1}{\epsilon_1} (v_1 - i\alpha)^2, \quad (17)$$

$$T_s(\alpha) = \frac{2}{\epsilon_1} v_1 (v_1 - i\alpha). \quad (18)$$

For a traveling incident wave, $0 \leq \alpha < n_1$, we have $\alpha = n_1 \sin \theta_i$ and $v_1 = n_1 \cos \theta_i$, with θ_i the angle of incidence. We can then write Eqs. (17) and (18) as

$$R_s(\alpha) = e^{-2i\theta_i}, \quad (tr), \quad (19)$$

$$T_s(\alpha) = 2 \cos \theta_i e^{-i\theta_i}, \quad (tr). \quad (20)$$

So R_s lies on the unit circle in the complex plane, and its magnitude is unity. For an evanescent incident wave, $\alpha > n_1$, R_s is real, and $-1 < R_s < 0$. Fig. 2 shows R_s in the complex plane. It can be shown from Eqs. (17) and (18) that

$$T_s(\alpha) = 1 + R_s(\alpha), \quad (21)$$

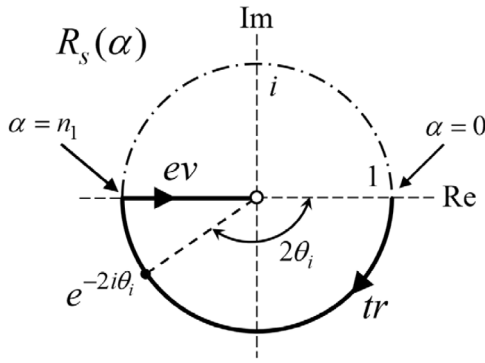


Fig. 2. The graph illustrates the values of R_s as a function of α in the complex plane.

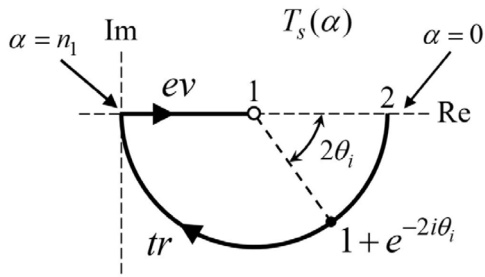


Fig. 3. Shown is the Fresnel transmission coefficient for s waves in the complex plane, as a function of α .

for all α . Fig. 3 shows T_s in the complex plane.

For p waves, we find immediately from Eq. (8)

$$R_p(\alpha) = -1, \tag{22}$$

since $\epsilon_2 = 0$. Unlike for s waves, the reflection coefficient does not depend on the angle of incidence for traveling waves, and the reflection coefficient for evanescent waves is unity in magnitude for all α . It seems to follow from Eq. (10) that $T_p = 0$ since $n_2 = 0$. However, for $\alpha = 0$ and $n_2 \neq 0$ we have $v_1 = n_1$ and $v_2 = n_2$ with Eq. (11). With $\epsilon_k = n_k^2$ this gives $T_p = 2n_1/(n_1 + n_2)$. For $n_2 \rightarrow 0$ this gives $T_p = 2$. We therefore conclude

$$\lim_{\epsilon_2 \rightarrow 0} T_p(\alpha) = \begin{cases} 2, & \alpha = 0 \\ 0, & \alpha \neq 0 \end{cases}. \tag{23}$$

It is interesting to notice that both for $\alpha \neq 0$ and $\alpha = 0$ the term $\epsilon_2 v_1$ in the denominator in Eq. (10) is always much smaller than the term $\epsilon_1 v_2$ for ϵ_2 small. Therefore

$$T_p(\alpha) \approx 2 \frac{v_1 n_2}{n_1 v_2}, \quad \epsilon_2 \text{ small}, \tag{24}$$

and in the limit $\epsilon_2 \rightarrow 0$ this becomes exact. Figs. 4 and 5 show the real and imaginary parts, respectively, of the exact T_p and its approximation by the right-hand side of Eq. (24). It appears that the approximation is near perfect. Eq. (24) will prove useful in the next section.

4. Fields

The reflected and transmitted electric and magnetic fields are expressed in terms of 15 auxiliary functions, listed in the Appendix. We now consider the limit $\epsilon_2 \rightarrow 0$ for these functions. For the reflected waves we substitute R_s and R_p from Eqs. (17) and (22) into Eq. (A.5) for the associated functions r_s and r_p . Nothing else simplifies for the r waves.

More interesting are the transmitted waves into the ENZ material. First, we have $v_2 = i\alpha$, and this factor appears in 3 integrands. It

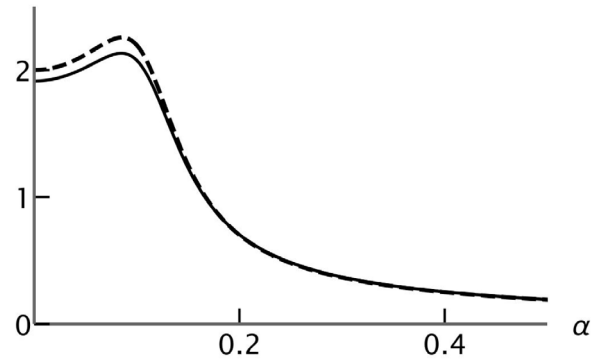


Fig. 4. The figure shows the real part of T_p (solid curve) and its approximation (dashed curve) by the real part of the right-hand side of Eq. (24) as a function of α . The parameters are $\epsilon_1 = 6$ and $\epsilon_2 = 0.01 * (1 + i)$.

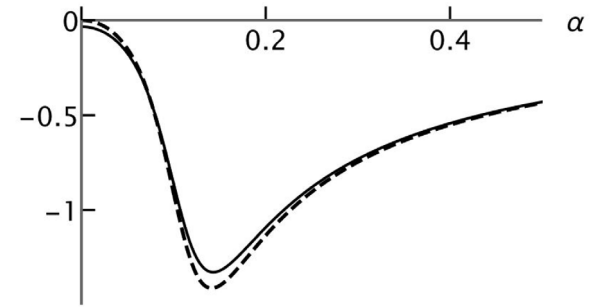


Fig. 5. The figure shows the imaginary part of T_p (solid curve) and its approximation (dashed curve) by the imaginary part of the right-hand side of Eq. (24) as a function of α . The parameters are $\epsilon_1 = 6$ and $\epsilon_2 = 0.01 * (1 + i)$.

also appears in the associated functions t_σ from Eq. (A.2), which now become

$$t_\sigma(\alpha, \bar{z}) = T_\sigma \frac{1}{v_1} e^{i v_1 h} e^{-\alpha \bar{z}}. \tag{25}$$

The \bar{z} dependence of the auxiliary functions only comes in through the associated functions, and we see that this as $\exp(-\alpha \bar{z})$. Therefore, all integrands decay exponentially in the positive z direction, corresponding to evanescent waves. This also shows that all $\mathcal{T}_\sigma^{(i)}$ functions have the form of a Laplace transform with \bar{z} as the Laplace parameter. Then we substitute Eq. (18) for T_s in t_s in Eq. (25). Next, for $\epsilon_2 \rightarrow 0$ we have $n_2 \rightarrow 0$, and this immediately gives

$$\mathcal{T}_p^{(7)}(\bar{\rho}, \bar{z}) = \mathcal{T}_p^{(8)}(\bar{\rho}, \bar{z}) = 0. \tag{26}$$

These functions only show up in Eq. (15) for the transmitted magnetic field, which now simplifies to

$$\tilde{\mathbf{B}}_t = -u_y \mathbf{e}_x \mathcal{T}_s^{(4)}. \tag{27}$$

The integrals $\mathcal{T}_p^{(i)}$ with $i = 1, 3, 4$ and 5 have an overall factor of $1/n_2$, which appears problematic for $n_2 \rightarrow 0$. However, they also have a factor T_p , which goes to zero with Eq. (23). Here we use Eq. (24) to find the limit $\epsilon_2 \rightarrow 0$ for these integrals. We have

$$\lim_{\epsilon_2 \rightarrow 0} \frac{\alpha}{n_1 n_2 v_1} T_p = -\frac{2i}{\epsilon_1}, \tag{28}$$

and in this fashion the limit exists. Now all dependence of the auxiliary functions on ϵ_2 has disappeared. This means that we do not just have ‘epsilon near zero’, but the limit $\epsilon_2 \rightarrow 0$.

5. Field lines of the Poynting vector

Electromagnetic energy flows along the field lines of the (time-averaged) Poynting vector, defined as

$$\mathbf{S}(\mathbf{r}) = \frac{1}{2\mu_0} \text{Re}[\mathbf{E}(\mathbf{r})^* \times \mathbf{B}(\mathbf{r})]. \quad (29)$$

We set

$$\mathbf{S}(\mathbf{r}) = S_0 \sigma(\mathbf{r}), \quad (30)$$

with

$$S_0 = \frac{\zeta^2}{2\mu_0 c}, \quad (31)$$

which gives

$$\sigma(\mathbf{r}) = \text{Re}[\tilde{\mathbf{E}}(\mathbf{r})^* \times \tilde{\mathbf{B}}(\mathbf{r})], \quad (32)$$

for the dimensionless Poynting vector σ in terms of the dimensionless fields. In region 1 the electric and magnetic fields are the sums of the source fields and the reflected fields, and in region 3 the fields are the transmitted fields.

Given the fields $\tilde{\mathbf{E}}$ and $\tilde{\mathbf{B}}$ found above, the Poynting vector in each region can be constructed and we can find field lines through given points by numerical integration. The only parameters left in the problem are ϵ_1 , h and the components u_y and u_z of the dipole moment polarization vector. For a linear dipole in the yz plane we can specify the angle γ with the positive z axis, rather than u_y and u_z separately. Then we have $u_y = \sin \gamma$ and $u_z = \cos \gamma$.

It can be shown on general grounds [25] that the total power crossing an ENZ interface (half-infinite medium) is zero for any choice of parameters. This does not mean that no power can cross the interface. When power crosses the interface at some point, it has to return to the lower medium at some other point. This oscillating of energy back and forth through an interface already happens when dipole radiation transmits into a thinner medium [24]. When a field line of energy flow enters the thinner medium, it bends away from the normal, similar to an optical ray, and if it bends enough, it can come back to the original medium. Apparently, an ENZ medium is the ultimate ‘thin’ medium, and all power eventually returns to the thicker medium where the dipole is located.

An example of energy flow is shown in Fig. 6 for a rotating dipole moment. The y axis is to the right, the z axis is up, and the dipole location is indicated by a black dot. The dipole moment rotates counterclockwise in the yz plane, and the field lines have a counterclockwise swirling appearance. We see on the left-hand side in the figure that the field lines bend away from the normal, and some return to the lower medium. Fig. 7 show a field line pattern for a linear dipole. On the right in the figure, energy is flowing along field lines running towards the interface. A circulation appears with a vortex at the center, indicated by a little circle. A second vortex appears along the dipole axis, just below the interface, and in between the vortices all energy is flowing from the ENZ medium into the dielectric. It is clear from Figs. 6 and 7 that energy flows into the ENZ material, and not only for field lines under normal incidence (as for *static optics*). Radiative energy penetrates the ENZ medium, and the field lines of energy flow connect smoothly with the field lines in the dielectric.

6. Perpendicular dipole

We now consider the simplest case of a dipole oscillating perpendicular to the surface. We then have $\hat{\mathbf{u}} = \mathbf{e}_z$, and the transmitted electric and magnetic fields become

$$\tilde{\mathbf{E}}_t = \mathbf{e}_z \mathcal{T}_p^{(3)} + \mathbf{e}_\rho \mathcal{T}_p^{(4)}, \quad (33)$$

$$\tilde{\mathbf{B}}_t = 0. \quad (34)$$

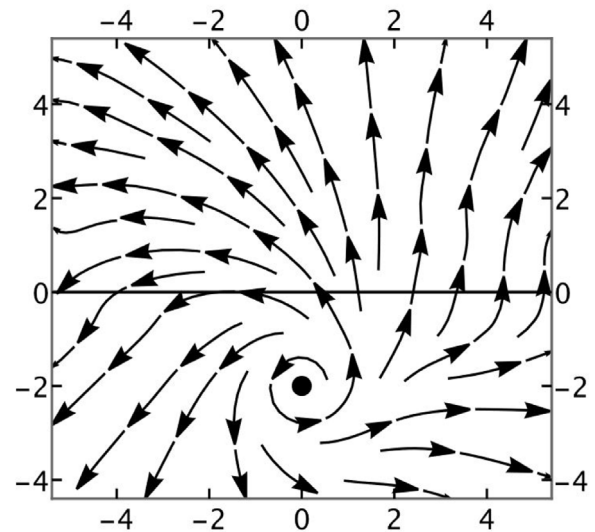


Fig. 6. The figure shows the flow lines of energy for a counterclockwise rotating dipole ($u_y = 1/\sqrt{2}$, $u_z = i/\sqrt{2}$) for $\epsilon_1 = 1$ and $h = 2$.

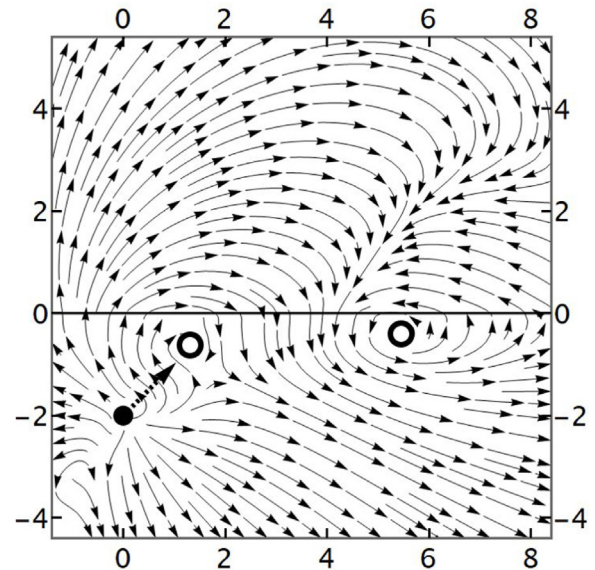


Fig. 7. Shown are the flow lines of energy for a linear dipole, oscillating under 45° with the z axis. The parameters are $\epsilon_1 = 1$ and $h = 2$.

Most notably, the magnetic field is identically zero in the ENZ medium, and therefore the Poynting vector is zero. There is no energy flow in the ENZ material. Fig. 8 shows the field lines of the Poynting vector for a perpendicular dipole. The field lines emanate from the dipole, but none of the field lines that go up enter the medium. On approach of the ENZ material, they bend, and flow away along the interface. It should be noted that for a perpendicular dipole the system is rotationally symmetric around the z axis, so the field lines off the yz plane, and in a plane through the z axis, are identical to the field lines in Fig. 8.

7. Electric field

Even though there is no magnetic field and no energy flow in the ENZ material for a perpendicular dipole, there is an electric field, given by Eq. (33). The time-dependent field is

$$\mathbf{E}(\mathbf{r}, t) = \zeta \text{Re}[\tilde{\mathbf{E}}(\mathbf{r}) e^{-i\omega t}], \quad (35)$$

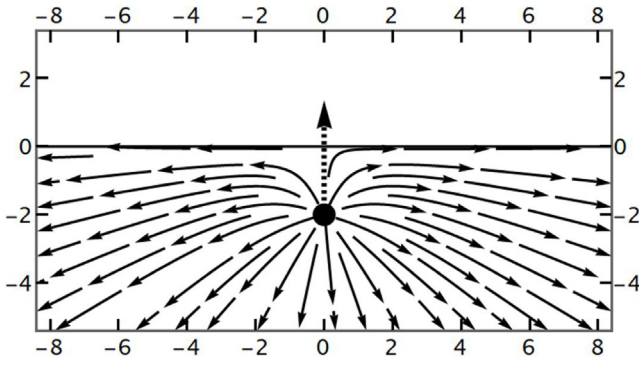


Fig. 8. The figure shows the flow line pattern for a perpendicular dipole. The parameters are $\epsilon_1 = 1$ and $h = 2$.

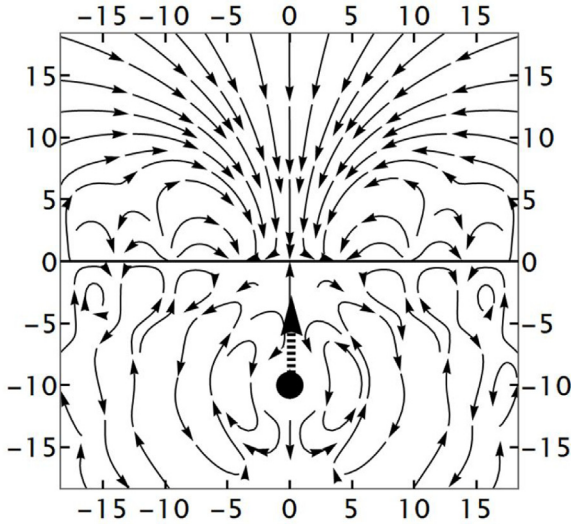


Fig. 9. The figure shows field lines of the electric field at $t = 0$ for $\epsilon_1 = 1$ and $h = 10$.

and so $\text{Re}[\tilde{\mathbf{E}}(\mathbf{r})]$ is the field at $t = 0$, apart from an overall constant. Fig. 9 shows the field lines of the electric field at $t = 0$. Near the dipole it has the familiar lobe structure. As seen from the figure, tiny vortices appear just below the interface on the left and the right in the picture. It seems that in the ENZ medium the field lines run predominantly towards the interface. However, the field is oscillating, so at a later time the field lines change direction.

Field lines of a vector field are determined by the direction of the field at each point, so the figures do not give any information about the strength of the field. In order to determine how rapidly the fields decay in the upward direction, we consider the limit $h \rightarrow 0$. The auxiliary functions in Eq. (33) become

$$T_p^{(3)}(\bar{\rho}, \bar{z}) = \frac{2}{\epsilon_1} \int_0^\infty d\alpha \alpha^2 e^{-\alpha \bar{z}} J_0(\alpha \bar{\rho}), \quad (36)$$

$$T_p^{(4)}(\bar{\rho}, \bar{z}) = \frac{2}{\epsilon_1} \int_0^\infty d\alpha \alpha^2 e^{-\alpha \bar{z}} J_1(\alpha \bar{\rho}), \quad (37)$$

and these can be evaluated in closed form. The result is

$$T_p^{(3)}(\bar{\rho}, \bar{z}) = \frac{2}{\epsilon_1} \frac{1}{q^5} (2\bar{z}^2 - \bar{\rho}^2), \quad (38)$$

$$T_p^{(4)}(\bar{\rho}, \bar{z}) = \frac{2}{\epsilon_1} \frac{1}{q^5} 3\bar{\rho}\bar{z}, \quad (39)$$

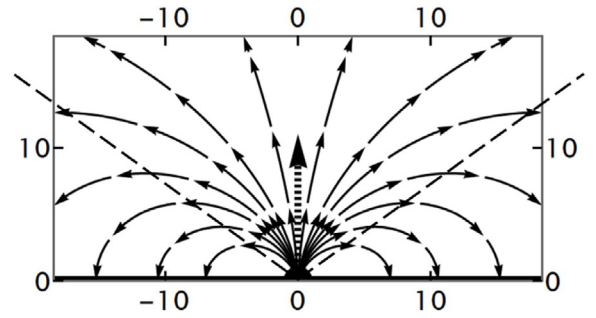


Fig. 10. Shown are the field lines of the electric field in the ENZ medium at $t = 0$ for $\epsilon_1 = 1$ and $h = 0$. Across the dashed lines the electric field is horizontal.

with

$$q = \sqrt{\bar{\rho}^2 + \bar{z}^2}, \quad (40)$$

as the dimensionless distance between the origin of coordinates and the field point. The complex amplitude of the electric field in the ENZ medium becomes

$$\tilde{\mathbf{E}}_t = \frac{2}{\epsilon_1} \frac{1}{q^5} [(2\bar{z}^2 - \bar{\rho}^2)\mathbf{e}_z + 3\bar{\rho}\bar{z}\mathbf{e}_\rho], \quad (41)$$

and this field is real. The ρ component is positive, so the vectors point away from the \bar{z} axis.

The z component changes sign at $\bar{z} = \bar{\rho}/\sqrt{2}$. For $\bar{z} < \bar{\rho}/\sqrt{2}$ the z component is negative, so the vectors point towards the interface, and for $\bar{z} > \bar{\rho}/\sqrt{2}$ the vectors point up. At the borderline $\bar{z} = \bar{\rho}/\sqrt{2}$ the electric field is horizontal. Fig. 10 shows the field lines, and the dashed lines are the $\bar{z} = \bar{\rho}/\sqrt{2}$ lines.

Of particular interest is the behavior of the field for large \bar{z} , so deep in the material. We find from Eq. (41)

$$\tilde{\mathbf{E}}_t = \frac{4}{\epsilon_1} \frac{1}{\bar{z}^3} \mathbf{e}_z + \dots \quad \bar{\rho} \text{ fixed, } \bar{z} \text{ large.} \quad (42)$$

The electric field is asymptotically in the positive z direction, and it falls off as $1/\bar{z}^3$. It is interesting to note that the integrals in Eqs. (36) and (37) are superpositions of evanescent waves, $\exp(-\alpha \bar{z})$. The sum, however, falls off algebraically as $1/\bar{z}^3$. All partial waves in the angular spectrum are evanescent, but their sum only decays algebraically, and has a long tail into the ENZ medium.

8. Conclusions

It is commonly perceived that no radiation can penetrate an ENZ material, except as evanescent waves. These waves decay exponentially with the distance to the interface, and propagate along the interface. An exception is *static optics*. A plane wave under normal incidence penetrates the medium. In the medium, an oscillating electric field exists, without spatial dependence, and no energy flow is associated with this electric field. We have considered electric dipole radiation, emitted near the interface with an ENZ medium. This radiation is a superposition of traveling and evanescent plane waves, and when incident upon the interface, all partial waves transmit as evanescent waves. The *static optics* waves do not contribute to the transmitted fields, because they have zero measure in an angular spectrum representation. We have evaluated the electric and magnetic fields in the ENZ medium, and we found that the limit $\epsilon_2 \rightarrow 0$ exists (due to the limit shown in Eq. (38)). Energy in the medium flows along the field lines of the Poynting vector, and typical examples of flow lines are shown in Figs. 6 and 7. In particular Fig. 7 shows clearly that energy which enters the medium at one point returns to the dielectric at another point. This should be so, because the total power crossing the interface is zero, on general grounds.

For a dipole oscillating perpendicular to the interface, no energy crosses the interface anywhere, as seen in Fig. 8. This is due to the fact that for this case the magnetic field in the ENZ medium is identically zero. There is, however, an electric field in the ENZ material, as illustrated in Figs. 9 and 10. For this situation, the electric field can be evaluated in closed form, and we found that it falls off as the third power of the distance to the interface. Apparently, the evanescent waves that make up this field add up to an algebraic decay. This seems counterintuitive, but this already happens for the electromagnetic Green's tensor in free space, and without any boundaries [26,27]. Along the z axis, the evanescent waves add up to a field that decays as $1/r$ in a cylindrical region around the z axis. For an ENZ medium, we have found that the evanescent waves of dipole radiation add up to algebraically decaying waves everywhere in the material. We have shown this explicitly for the electric field of a perpendicular dipole, but this holds in general for the electric and magnetic fields of a dipole with arbitrary orientation. Then also a magnetic field penetrates the material, and consequently there is an energy flow throughout the ENZ medium, as illustrated in Figs. 6 and 7.

Declaration of competing interest

The authors declare that they have no known competing financial interests or personal relationships that could have appeared to influence the work reported in this paper.

Acknowledgment

This research did not receive any specific grant from funding agencies in the public, commercial, or not-for-profit sectors.

Appendix. Single interface formulas

Here we list the necessary formulas for the solution for an interface with a medium of arbitrary ε_2 , and for a field point in the yz plane. The associated functions are defined as

$$r_\sigma(\alpha, \bar{z}) = R_\sigma e^{i v_1(h-\bar{z})}, \quad (\text{A.1})$$

$$t_\sigma(\alpha, \bar{z}) = T_\sigma \frac{1}{v_1} e^{i(v_1 h + v_2 \bar{z})}, \quad (\text{A.2})$$

with $\sigma = s, p$. The needed auxiliary functions are

$$\mathcal{R}_s^{(1)}(\bar{\rho}, \bar{z}) = \frac{i}{2} \int_0^\infty d\alpha \frac{\alpha}{v_1} r_s (J_0 + J_2), \quad (\text{A.3})$$

$$\mathcal{R}_s^{(4)}(\bar{\rho}, \bar{z}) = -\frac{i}{2} \int_0^\infty d\alpha \alpha r_s v_1 (J_0 + J_2), \quad (\text{A.4})$$

$$\mathcal{T}_s^{(1)}(\bar{\rho}, \bar{z}) = \frac{i}{2} \int_0^\infty d\alpha \alpha t_s (J_0 + J_2), \quad (\text{A.5})$$

$$\mathcal{T}_s^{(4)}(\bar{\rho}, \bar{z}) = \frac{i}{2} \int_0^\infty d\alpha \alpha t_s v_2 (J_0 + J_2), \quad (\text{A.6})$$

$$\mathcal{R}_p^{(1)}(\bar{\rho}, \bar{z}) = -\frac{i}{2n_1^2} \int_0^\infty d\alpha \alpha r_p v_1 (J_0 - J_2), \quad (\text{A.7})$$

$$\mathcal{R}_p^{(3)}(\bar{\rho}, \bar{z}) = \frac{i}{n_1^2} \int_0^\infty d\alpha \frac{\alpha}{v_1} r_p \alpha^2 J_0, \quad (\text{A.8})$$

$$\mathcal{R}_p^{(4)}(\bar{\rho}, \bar{z}) = -\frac{1}{n_1^2} \int_0^\infty d\alpha \alpha r_p \alpha J_1, \quad (\text{A.9})$$

$$\mathcal{R}_p^{(6)}(\bar{\rho}, \bar{z}) = \frac{i}{2} \int_0^\infty d\alpha \alpha r_p (J_0 - J_2), \quad (\text{A.10})$$

$$\mathcal{R}_p^{(7)}(\bar{\rho}, \bar{z}) = \int_0^\infty d\alpha \frac{\alpha}{v_1} r_p \alpha J_1, \quad (\text{A.11})$$

$$\mathcal{T}_p^{(1)}(\bar{\rho}, \bar{z}) = \frac{i}{2n_1 n_2} \int_0^\infty d\alpha \alpha t_p v_1 v_2 (J_0 - J_2), \quad (\text{A.12})$$

$$\mathcal{T}_p^{(3)}(\bar{\rho}, \bar{z}) = \frac{i}{n_1 n_2} \int_0^\infty d\alpha \alpha t_p \alpha^2 J_0, \quad (\text{A.13})$$

$$\mathcal{T}_p^{(4)}(\bar{\rho}, \bar{z}) = \frac{1}{n_1 n_2} \int_0^\infty d\alpha \alpha t_p \alpha v_2 J_1, \quad (\text{A.14})$$

$$\mathcal{T}_p^{(5)}(\bar{\rho}, \bar{z}) = \frac{1}{n_1 n_2} \int_0^\infty d\alpha \alpha t_p \alpha v_1 J_1, \quad (\text{A.15})$$

$$\mathcal{T}_p^{(7)}(\bar{\rho}, \bar{z}) = \frac{i n_2}{2n_1} \int_0^\infty d\alpha \alpha t_p v_1 (J_0 - J_2), \quad (\text{A.16})$$

$$\mathcal{T}_p^{(8)}(\bar{\rho}, \bar{z}) = \frac{n_2}{n_1} \int_0^\infty d\alpha \alpha t_p \alpha J_1. \quad (\text{A.17})$$

Here, $J_k = J_k(\alpha \bar{\rho})$. The numerical evaluation of these integrals is far from trivial, partially because of the factor $1/v_1$ in several integrands. We have $v_1 = 0$ for $\alpha = n_1$, so some integrands have a singularity on the integration axis. Furthermore, v_1 has a branch point at $\alpha = n_1$, and this branch point appears in exponents in Eqs. (A.1) and (A.2). These singularities and branch points can be transformed away by splitting the integrals in their traveling (range $0 \leq \alpha < n_1$) and evanescent (range $n_1 < \alpha < \infty$) parts, and then make a change of variables in each [28].

References

- [1] Z. Xu, H.F. Arnoldus, *OSA Cont.* 2 (2019) 722.
- [2] M.G. Silveirinha, N. Engheta, *Phys. Rev. Lett.* 97 (2006) 157403.
- [3] M.G. Silveirinha, N. Engheta, *Phys. Rev. B* 76 (2007) 245109.
- [4] A. Alù, N. Engheta, *Phys. Rev. B* 78 (2008) 035440.
- [5] D.A. Powell, A. Alù, B. Edwards, A. Vakil, Y.S. Kivshar, N. Engheta, *Phys. Rev. B* 79 (2009) 245135.
- [6] B. Edwards, A. Alù, M.G. Silveirinha, N. Engheta, *J. Appl. Phys.* 105 (2009) 044905.
- [7] A. Alù, N. Engheta, *IEEE Trans. Antennas Propag.* 58 (2010) 328.
- [8] S. Enoch, G. Tayeb, P. Sabouroux, N. Guerin, P. Vincent, *Phys. Rev. Lett.* 89 (2002) 213902.
- [9] A. Alù, M.G. Silveirinha, A. Salandrino, N. Engheta, *Phys. Rev. B* 75 (2007) 155410.
- [10] B. Wang, K.-M. Huang, *Prog. Electr. Res.* 106 (2010) 107.
- [11] L.V. Alekseyev, E.E. Narimanov, T. Tumkur, H. Li, Y.A. Barnakov, M.A. Noginov, *Appl. Phys. Lett.* 106 (2010) 107.
- [12] J.A. Girón-Sedas, J.R. Mejía-Salazar, J.C. Granada, O.N. Oliveira, *Phys. Rev. B* 94 (2016) 245430.
- [13] F.J. Rodríguez-Fortuño, M.F. Picardi, A.V. Zayats, *Phys. Rev. B* 97 (2018) 205401.
- [14] F.J. Rodríguez-Fortuño, A. Vakil, N. Engheta, *Phys. Rev. Lett.* 112 (2014) 033902.
- [15] H.F. Arnoldus, Z. Xu, *J. Opt. Soc. Amer. B* 36 (2019) F18.
- [16] B. Edwards, A. Alù, M.E. Young, M.G. Silveirinha, N. Engheta, *Phys. Rev. Lett.* 100 (2008) 033903.
- [17] H. Lobato-Morales, D.V.B. Murthy, A. Corona-Chávez, J.L. Olvera-Cervantes, L.G. Guerrero-Ojeda, *IEEE Trans. Microw. Theory Tech.* 59 (2011) 1863.
- [18] V. Torres, B. Orzabayev, V. Pacheco-Peña, J. Teniente, M. Beruete, M. Navarro-Cía, M.S. Ayzza, N. Engheta, *IEEE Trans. Antennas Propag.* 63 (2015) 231.
- [19] M. Massauti, A.A. Basharin, M. Kafesaki, M.F. Acosta, R.I. Merino, V.M. Orera, E.N. Economou, C.M. Soukoulis, S. Tzortzakakis, *Opt. Lett.* 38 (2013) 1140.
- [20] V. Pacheco-Peña, N. Engheta, S. Kuznetsov, A. Gentsel, M. Beruete, *Phys. Rev. Appl.* 8 (2017) 034036.
- [21] B.T. Schwartz, R. Piestun, *J. Opt. Soc. Amer. B* 20 (2003) 2448.
- [22] R. Maas, J. Parsons, N. Engheta, *Nature Photon.* 7 (2013) 907.
- [23] E.J.R. Vesseur, T. Coenen, H. Caglayan, N. Engheta, A. Polman, *Phys. Rev. Lett.* 110 (2013) 013902.
- [24] H.F. Arnoldus, M.J. Berg, *J. Modern Opt.* 62 (2015) 244.
- [25] Z. Xu, H.F. Arnoldus, *J. Modern Opt.* 66 (2019) 2043.
- [26] H.F. Arnoldus, J.T. Foley, *J. Opt. Soc. Amer. A* 19 (2002) 1701.
- [27] H.F. Arnoldus, *Advances in Imaging and Electron Physics* 132, Elsevier Academic Press, New York, Ed. Peter W. Hawkes, 2004, p. 1.
- [28] H.F. Arnoldus, *Comput. Phys. Comm.* 257 (2020) 107510.